UC Davis
UC Davis Previously Published Works

Title

Fructose-induced hypertriglyceridemia in rhesus macaques is attenuated with fish oil or ApoC3 RNA interference[S]

Permalink

Journal

ISSN

Authors

Butler, Andrew A
Price, Candice A
Graham, James L
et al.

Publication Date

DOI

Peer reviewed

Fructose-induced hypertriglyceridemia in rhesus macaques is attenuated with fish oil or ApoC3 RNA interference[s]

Andrew A. Butler,* Candice A. Price,[†] James L. Graham,[†] Kimber L. Stanhope,[†] Sarah King,[§] Yu-Han Hung,** Praveen Sethupathy,** So Wong,[††] James Hamilton,[††] Ronald M. Krauss,[§] Andrew A. Bremer,[§§] and Peter J. Havel[1,†]

Department of Pharmacology and Physiology,* Saint Louis University School of Medicine, St. Louis, MO; Department of Molecular Biosciences,[†] School of Veterinary Medicine, California National Primate Research Center, and Department of Nutrition, University of California, Davis, CA; Children's Hospital Oakland Research Institute,[§] Oakland, CA; Department of Biomedical Sciences,** College of Veterinary Medicine, Cornell University, Ithaca, NY; Arrowhead Pharmaceuticals,[††] Pasadena, CA; and Department of Pediatrics,[§§] Vanderbilt University, Nashville, TN

Abstract Dyslipidemia and insulin resistance are significant adverse outcomes of consuming high-sugar diets. Conversely, dietary fish oil (FO) reduces plasma lipids. Diet-induced dyslipidemia in a rhesus model better approximates the pathophysiology of human metabolic syndrome (MetS) than rodent models. Here, we investigated relationships between metabolic parameters and hypertriglyceridemia in rhesus macaques consuming a high-fructose diet (n = 59) and determined the effects of FO supplementation or RNA interference (RNAi) on plasma ApoC3 and triglyceride (TG) concentrations. Fructose supplementation increased body weight, fasting insulin, leptin, TGs, and large VLDL particles and reduced adiponectin concentrations (all *P* < 0.001). In multiple regression analyses, increased plasma ApoC3 was the most consistent and significant variable related to diet-induced hypertriglyceridemia. FO supplementation, which attenuated increases of plasma TG and ApoC3 concentrations, reversed fructose-induced shifts of lipoprotein particle size toward IDL and VLDL, a likely mechanism contributing to beneficial metabolic effects, and reduced hepatic expression of genes regulated by the SREBP pathway, particularly acetyl-CoA carboxylase. Furthermore, RNAi-mediated ApoC3 inhibition lowered plasma TG concentrations in animals with diet-induced hypertriglyceridemia. [jlr] In summary, ApoC3 is an important independent correlate of TG-rich lipoprotein concentrations in rhesus macaques consuming a high-fructose diet. ApoC3 is a promising therapeutic target for hypertriglyceridemia in patients with MetS and diabetes.—Butler, A. A., C. A. Price, J. L. Graham, K. L. Stanhope, S. King, Y-H. Hung, P. Sethupathy, S. Wong, J. Hamilton, R. M. Krauss, A. A. Bremer, and P. J. Havel. **Fructose-induced hypertriglyceridemia in rhesus macaques is attenuated with fish oil or ApoC3 RNA interference.** *J. Lipid Res.* 2019. **60:** 805–818.

Supplementary key words diet effects/lipid metabolism • nutrition/carbohydrate • nonhuman primate models • apolipoproteins • ribonucleic acid interference • lipogenic enzymes • acetyl-coenzyme A carboxylase • apolipoprotein C3

Elevation of cholesterol and/or triglycerides (TGs) in the circulation (dyslipidemia) is a frequent but modifiable risk factor for CVD (1, 2). Inhibition of cholesterol synthesis using HMG-CoA reductase inhibitors (statins) is considered a first line of treatment for dyslipidemias involving elevated levels of LDL cholesterol (LDL-C). However, effective treatments for dyslipidemias in situations of statin-resistance or intolerance, or that involve severe hyperglyceridemia,

have been achieved using therapies targeting lipoprotein metabolism (3). These treatments have been aimed at modifying the transport of lipids in the circulatory and lymphatic systems, which is directed via trafficking in lipid-protein (lipoprotein) complexes (2). Apolipoproteins possessing both hydrophobic and hydrophilic (amphipathic) properties are embedded in a membrane that surrounds a hydrophobic lipid core. Apolipoproteins situated in the outer membrane act as ligands for cell-surface receptors that direct lipoprotein uptake to specific cell-types, and also regulate lipase-dependent release of TG (2).

ApoC3 is considered a highly promising candidate for treating severe hypertriglyceridemia (4, 5). Loss-of-function mutations in the *APOC3* gene are associated with lower fasting and postprandial TG concentration, reduced LDL-C concentrations, increased HDL cholesterol (HDL-C) concentrations, and a substantially (~40%) reduced risk of CVD (6–9). In contrast, transgenic mice overexpressing ApoC3 exhibit hypertriglyceridemia (10, 11). Clinical studies in which ApoC3 synthesis is suppressed by antisense oligonucleotides (volanesorsen, Ionis 304801) have demonstrated substantial TG-lowering effects in patients with severe hypertriglyceridemia (12, 13).

Incorporating fish oils (FOs) that are rich sources of the two major n-3 (ω-3) PUFAs, EPA and DHA, into the diet has long been implicated in a reduced risk for CVD (14). FOs as dietary supplements providing EPA alone, and in combination with DHA, reduced risk of CVD in several randomized controlled trials (15). The anti-hyperlipidemic actions of FOs result from reduced de novo lipogenesis and hepatic production of VLDL cholesterol (VLDL-C) (16).

The current study extends our analysis of a nonhuman primate (rhesus macaque) model of diet-induced insulin resistance and dyslipidemia using nonhuman primates (rhesus macaques) (17). Nonhuman primates have a number of clear advantages over more commonly used rodent models of metabolic disease. They are more closely related evolutionarily and have metabolic physiology and lipid metabolism that are more similar to that in humans (18, 19). Rhesus macaques provided with fructose-sweetened beverages rapidly develop insulin resistance, hypertriglyceridemia, and inflammation (17). FO supplements prevent the concurrent increases of both plasma ApoC3 and TG concentrations in animals provided fructose-sweetened beverages (20). In this study, we investigated the relationships between ApoC3 and dyslipidemia in a large cohort (n = 59) of rhesus macaques with fructose-induced dyslipidemia and insulin resistance. We also report results from this model investigating the effects of a novel RNA interference (RNAi) technology that targets ApoC3, and further explored the impact of FO supplementation on lipoprotein particle size distribution and the expression of genes involved in hepatic lipid/lipoprotein metabolism.

MATERIALS AND METHODS

Rhesus macaques

Adult male rhesus macaques (n = 59) (age 12.0 ± 2.8 years, range 6.4–17.8) maintained at the California National Primate

Research Center (CNPRC) were allowed ad libitum access to a standard commercial nonhuman primate diet (Advanced Protocol Old World Primate, LabDiet 5047) and water. This is primarily a grain-based diet that provides 30%/kcal as protein, 11%/kcal as fat, and 59%/kcal in the form of carbohydrates.

After determination of baseline body weight and collection of fasting blood samples, animals were provided a 15% fructose solution [75 g/day of fructose (~300 kcal) in 500 ml/day of flavored Kool-Aid, Kraft Foods] for a 3 month time period. Male rhesus macaques consume on average 800–900 kcal/day, so these animals received approximately 30% of energy from fructose (17). Animals were weighed and fasting blood samples were collected again after 1 and 3 months of fructose consumption.

Ten additional adult male fructose-fed rhesus monkeys were supplemented with 4 g/day of whole FO (Jedwards, Inc., Braintree, MA) for 6 months. The lipoprotein particle size results from these animals were compared with those from a subset of nine contemporaneously studied animals from the n = 59 group (20). Protocols for all the animal studies were approved by the University of California, Davis, Institutional Animal Care and Use Committee and were conducted in accordance with the US Department of Agriculture Animal Welfare Act and the National Institutes of Health's *Guide for the Care and Use of Laboratory Animals.*

ApoC3 RNAi study

The 20 animals used for these experiments received a modified moderate fat diet protocol and supplementation with high-fructose corn syrup (HFCS) in order to more closely match a human diet as well as maximize hypertriglyceridemia. Rhesus macaques received HFCS-sweetened beverage (500 ml, 15% by weight sugar) twice per day, receiving a total of 150 g (600 kcal) of HFCS [~55% fructose (330 kcal) and ~45% glucose (270 kcal)] per day. These animals may have received up to 60% of their calories as sugar. These animals were maintained on New World monkey diet (LabDiet 5040), which has a moderate fat content (~23% kcal). Plasma samples (fasting) were collected at baseline. The animals were then started on the HFCS diet for 5 weeks. After 5 weeks on the moderate fat/HFCS diet, an RNAi trigger targeting *APOC3* mRNA (ARO-APOC3, 4 mg/kg) was administered in four animals via subcutaneous injection on day 0 and day 29 (n = 4). Two additional animals received vehicle injections.

ARO-APOC3 is a synthetic double-stranded (both strands contain 21 nucleotides) hepatocyte-targeted *N*-acetylgalactosamine-conjugated RNAi trigger molecule. The *N*-acetylgalactosamine moiety targets the RNAi triggers to hepatocytes by acting as a ligand for the highly expressed hepatocyte-specific asialoglycoprotein receptor. The RNAi trigger was designed to silence APOC3 mRNA in humans and nonhuman primates with high specificity. The RNAi trigger was synthesized with 2′-O-methyl/2′-fluoro-modified nucleotides to provide nuclease resistance and to abrogate potential immune activation (21). Fasting blood samples were then collected for the measurement of plasma ApoC3 and TG at days 8, 15, 21, 29, 36, 43, 50, 57, 71, and 85. Several nonfasting blood samples were collected at baseline before the diet, prior to the RNAi or vehicle injections, and at days 7, 28, 56, and 84 following the injections.

FO study

For the experiment comparing the effects of FO with control oil on hepatic gene expression, 14 animals were maintained on the same HFCS beverage regimen used for the ARO-APOC3 experiment and provided a moderate fat (~36% kcal) typical American diet (TestDiet, TAD #5L0P) specifically modified to have FO and fructose removed from the formulation. The animals were on the diet for 1.5–2.5 months prior to treatment. Animals were

selected to either receive 4 g/day of FO (Jedwards, Inc.) or 4 g/day of a control oil (BestBlend®; Wesson, Inc., Memphis, TN) containing a mixture of soybean and canola oils providing approximately 40% of fat calories as polyunsaturated fat, 40% as monounsaturated fat, and 10% as saturated fat for 4 weeks. Diet composition and certificates of analysis are provided as supplemental information. The fish and control oil were stored in containers at 4°C under nitrogen gas to limit oxidation.

After 4 weeks of supplementation, the animals were anesthetized with isoflurane and 10–15 small laparoscopic liver biopsy samples were taken. A laparoscopic surgical liver biopsy procedure was performed by veterinary staff in a surgical suite at the CNPRC in overnight-fasted animals between 8:00 AM and 9:00 AM. Animals were sedated with ketamine (5–30 mg/kg im), intubated, and prepared for surgery. Anesthesia was maintained using inhalant anesthesia (1–3% isoflurane). A series of two to three small (∼1 cm) incisions were made through the skin and subcutaneous tissues into the abdomen. Laparoscopy tools were inserted to visualize the area of dissection, followed by introduction of a Veress needle and insufflation of the abdomen. Up to 10 (∼2–3 mm cubed) small liver samples were extracted using biopsy forceps and frozen in liquid nitrogen. Biopsy samples were aliquoted into three different tubes and snap-frozen in liquid nitrogen. The abdomen was closed using suture in two layers, and the animals were allowed to recover from anesthesia. For postoperative monitoring the monkeys were observed continuously until conscious, and then checked regularly until fully recovered by the CNPRC primate medicine staff. Animals were monitored postoperatively for signs of pain or bleeding for several days. Postoperative analgesia employed buprenorphine 0.03 mg/kg administered twice daily by intramuscular injection and ketoprofen (5 mg/kg im, daily) for 3 days post procedure.

Measurement of metabolites, lipoproteins, and apolipoproteins

Plasma glucose concentrations were measured with a YSI glucose analyzer (YSI Life Sciences). Plasma total cholesterol (TC), HDL-C, direct LDL-C, TG, ApoA1, ApoB, ApoC3, and ApoE concentrations were determined by using a Polychem chemistry analyzer (PolyMedCo) with reagents from MedTest DX (Canton, MI). VLDL-C was calculated by subtracting HDL-C and LDL-C from TC. Plasma concentrations of LDL-C and ApoB determined using these assays were highly correlated ($R^2 = 0.67$ at baseline, $R^2 = 0.69$ after 1 month, and $R^2 = 0.79$ after 3 months of fructose consumption) and changes (Δs) of LDL-C and ApoB were also highly correlated at 1 month ($R^2 = 0.53$) and 3 months ($R^2 = 0.59$) post fructose consumption (supplemental Fig. S1), indicating that while ApoB was not increased in rhesus macaques on the high-fructose diet, this is not likely due to a lack of specificity or sensitivity of the assay used for ApoB. The lipoprotein particle size separation assays and the anti-apolipoprotein antibody assays were developed for use in human samples, and have not been specifically validated for use in monkey plasma.

Concentrations of VLDL, IDL, LDL, and HDL particle subfractions were further analyzed in specific particle-size intervals using ion mobility, which uniquely allows for direct particle quantification as a function of particle diameter (22), following a procedure to remove other plasma proteins (23). The ion mobility instrument utilizes an electrospray to create an aerosol of particles, which then pass through a differential mobility analyzer coupled to a particle counter. Particle concentrations (in nanomoles per liter) are determined for subfractions defined by the following size intervals: VLDL: large (42.40–54.70 nm), medium (33.50–42.39 nm), small (29.60–33.49 nm); IDL: large (25.00–29.59 nm), small (23.33–24.99 nm); LDL: large (22.0–23.32 nm), medium (21.41–21.99 nm), small (20.82–21.40 nm), very small (18.0–20.81 nm); HDL: large (10.50–14.50 nm); small (7.65–10.49 nm). Peak LDL diameter (in nanometers) was determined as previously described (22).

Measurement of pancreatic and adipocyte hormones

Plasma adiponectin, insulin. and leptin concentrations were determined by RIA with assays from Millipore (Burlington, MA).

RNA-seq analysis of gene expression in liver biopsy samples

Total RNA was isolated from liver biopsies using the Norgen total RNA purification kit (Norgen Biotek, Thorold, ON, Canada). RNA quality was assessed by NanoDrop (ThermoFisher Scienctific, Waltham, MA) and RNA integrity was measured by TapeStation software (Agilent Technologies, Santa Clara, CA). Sequencing libraries were generated using the Illumina TruSeq polyA+ sample prep kit and single-end sequenced (50 times) on the HiSeq platform. Sequencing reads were mapped to the human genome using STAR (v2.5.3a) and transcripts/genes were quantified using Salmon (v0.6.0). The mapping rate averaged ∼60% across all samples. Differential gene expression analysis was performed using DESeq2.

For quantitation using quantitative (q)RT-PCR, a high-capacity RNA to cDNA kit (Life Technologies, Grand Island, NY) was used for reverse transcription of RNA. Acetyl-CoA carboxylase (ACACA) gene expression quantitative PCR was performed using TaqMan assays per the manufacturer's protocol on a Bio-Rad CFX96 Touch real-time PCR detection system (Bio-Rad Laboratories, Richmond, CA). Reactions were performed in triplicate using RPS9 as the normalizer.

Statistical analysis

Descriptive statistics are provided for each of the outcomes as mean ± SEM. Analysis for significance used SPSS Statistic version 24 (IBM). The effects of diet on each outcome parameter were initially compared with repeated measures nonparametric test (Friedman). Relationships between changes of TG, ApoC3, ApoE, and HOMA-IR were examined with simple and multivariate regression analyses using log-transformed data.

For the effects of RNAi treatment with ARO-APOC3 on plasma ApoC3 and TG concentrations in animals with HFCS-induced hypertriglyceridemia, we compared the mean of concentrations from day 43 to day 85 time points during which fasting plasma ApoC3 and fasting and nonfasting TG concentrations were stable versus day 8 ("baseline"). Paired t-tests were performed to determine the effects of ARO-APOC3 versus baseline pretreatment concentrations.

RESULTS

Effect of fructose consumption on body weight and metabolic outcomes

The effects of fructose consumption for 1 and 3 months on body weight and indices of glucose homeostasis (fasting glucose, insulin, and HOMA-IR), leptin, and adiponectin concentrations in rhesus macaques are summarized in **Table 1**. Rhesus macaques provided with fructose-sweetened beverages progressively increased weight over time (diet effect, $P < 0.001$). Overall, fructose consumption rapidly induced a state of insulin resistance and changes of circulating adipokines that are indicative of disrupted metabolic homeostasis. Rapid effects of diet were observed on fasting

TABLE 1. Impact of dietary supplementation with fructose on body weight and indices of glucose homeostasis

	Prefructose Measurement	1 Month Fructose Measurement (Change)	3 Months Fructose Measurement (Change)	Diet Effect*
Body weight (kg)	15.9 ± 0.3	16.7 ± 0.3^a (+0.8 ± 0.1)	17.5 ± 0.3^b (+1.6 ± 0.1**)	$P < 0.001$
Glucose (mg/dl)	80 ± 2	78 ± 2 (−2 ± 2)	77 ± 2 (−3 ± 2)	$P < 0.05$
Insulin (μ/ml)	66 ± 7	109 ± 15^c (+44 ± 111)	129 ± 26^d (+63 ± 195)	$P < 0.001$
HOMA-IR	13.2 ± 1.4	21.5 ± 3.2^c (+8.4 ± 3.1)	25.2 ± 5.5^d (+12.1 ± 5.4)	$P < 0.01$
Leptin (ng/ml)	19.7 ± 1.5	23.1 ± 1.6^e (+3.3 ± 0.6)	24.8 ± 1.6^f (+5.0 ± 0.9*)	$P < 0.001$
Adiponectin (μg/ml)	9.3 ± 1.0	6.7 ± 0.7^e (−2.6 ± 0.4)	6.1 ± 0.6^f (−3.2 ± 0.6*)	$P < 0.001$

In the third and fourth columns, changes in concentration (Conc.) are in parentheses. The significance between measurements before and during fructose consumption determined using post hoc comparisons are indicated by superscript letters: [a]$P < 0.001$ versus prefructose, 3 months fructose; [b]$P < 0.001$ versus prefructose, 1 month fructose; [c]$P < 0.01$ versus prefructose; [d]$P < 0.05$ versus prefructose; [e]$P < 0.001$ versus prefructose, $P < 0.05$ versus 3 months fructose; [f]$P < 0.001$ versus prefructose, $P < 0.05$ versus 1 month fructose.
*$P \leq 0.05$, significant difference between deltas at 1 and 3 months.
**$P < 0.001$, significant difference between deltas at 1 and 3 months.

insulin concentrations ($P < 0.001$) and HOMA-IR ($P < 0.01$), suggesting the development of insulin resistance (Table 1). The increase of HOMA-IR was primarily the result of increased plasma insulin concentrations, with fasting glucose concentrations exhibiting small but significant decreases (Table 1).

Leptin resistance and reduced adiponectin signaling contribute to metabolic dysfunction in obesity (24). Fasting plasma leptin concentrations rapidly increased during fructose consumption, while fasting adiponectin concentrations declined at 1 and 3 months (Table 1). Increases of fasting leptin were correlated with weight gain after 3 months of fructose consumption ($\rho = 0.392$, $P < 0.01$). However, the observed changes of indices of insulin resistance (fasting plasma insulin or HOMA-IR) were not correlated with baseline or fructose-induced changes of plasma leptin or adiponectin concentrations.

Effect of fructose consumption on plasma lipid and lipoprotein concentrations

Consumption of fructose-sweetened beverages produced marked increases of fasting TG and VLDL-C concentrations (**Fig. 1A**) (diet effect for both measurements, $P < 0.001$). Fasting TG concentrations increased by approximately 100% over baseline concentrations after 1 month of fructose consumption. VLDL-C levels increased approximately 70% over baseline concentrations (Fig. 1B).

Fructose consumption increased circulating TC by ~10% ($P < 0.005$). Small differences in HDL-C were also observed (diet effect, $P < 0.05$); however, HDL-C was not significantly changed compared with baseline after 3 months. Mean LDL-C concentrations were not significantly affected by consumption of the high-fructose diet.

For the apolipoproteins, the most marked effects of fructose intake were observed for ApoC3 and ApoE (diet effects, both $P < 0.001$). These responses to fructose consumption were rapid and similar to the increases observed for TG and VLDL-C. Increases of ApoC3 and ApoE concentrations peaked after 1 month, with no further increases after 3 months of fructose consumption. Both ApoC3 and ApoE increased approximately 40% during the diet (Fig. 1C, D), with strong correlations with each other ($\rho = 0.501$, $P < 0.001$). While the fructose-sweetened beverage had a

significant effect on ApoA1 ($P < 0.05$), the effects were small and not consistent over time (Fig. 1C, D). Fructose consumption had no significant effect on plasma ApoB concentrations (Fig. 1C, D).

Fructose rapidly increases plasma lipoproteins in rhesus macaques

Type 2 diabetes and the metabolic syndrome (MetS) are associated with increased small dense LDL-C and large-diameter TG-enriched VLDL-C levels (25). Fructose consumption had significant effects to increase circulating levels of most lipoprotein particles fractionated by particle diameter (**Table 2**). Repeated measures analysis using pooled LDL, IDL, and VLDL data indicated significant effects of diet (LDL, $P < 0.05$; for IDL and VLDL, $P < 0.001$). However, proportionately, fructose consumption appears to have a greater impact to increase the larger lipoprotein particles (Fig. 1E).

Fasting TG concentrations were highly correlated with VLDL subfractions (**Fig. 2A**–C). Relationships between VLDL-C and VLDL subfractions were not observed in chow-fed condition (Fig. 2D–F); however, VLDL-C exhibited strong correlations with VLDL subfractions after 3 months on the high-fructose diet (Fig. 2G–I). A robust relationship also developed between fasting TG and VLDL-C concentrations during the 3 months of fructose consumption (supplemental Fig. S2) ($\rho = 0.356$ at baseline, $\rho = 0.647$ after 3 months, both $P < 0.01$). Indeed, fructose consumption had similar effects to increase both fasting TG and VLDL-C concentrations (Fig. 1B). Increases (Δ) of circulating TG and VLDL-C levels were also highly correlated after 1 and 3 months of fructose consumption ($\rho = 0.73$ and 0.71, $P < 0.01$).

Correlation between fructose-induced hypertriglyceridemia and ApoC3

We next used simple and multiple regression modeling to identify variables closely related to fructose-induced increases of fasting TG, IDL, and VLDL particles after 1 and 3 months of fructose consumption. Independent variables used in the analysis were initially selected based on indices of glucose and lipid homeostasis exhibiting physiologically significant responses to diet (Table 1, Fig. 1C). Baseline values were included in the model to assess whether
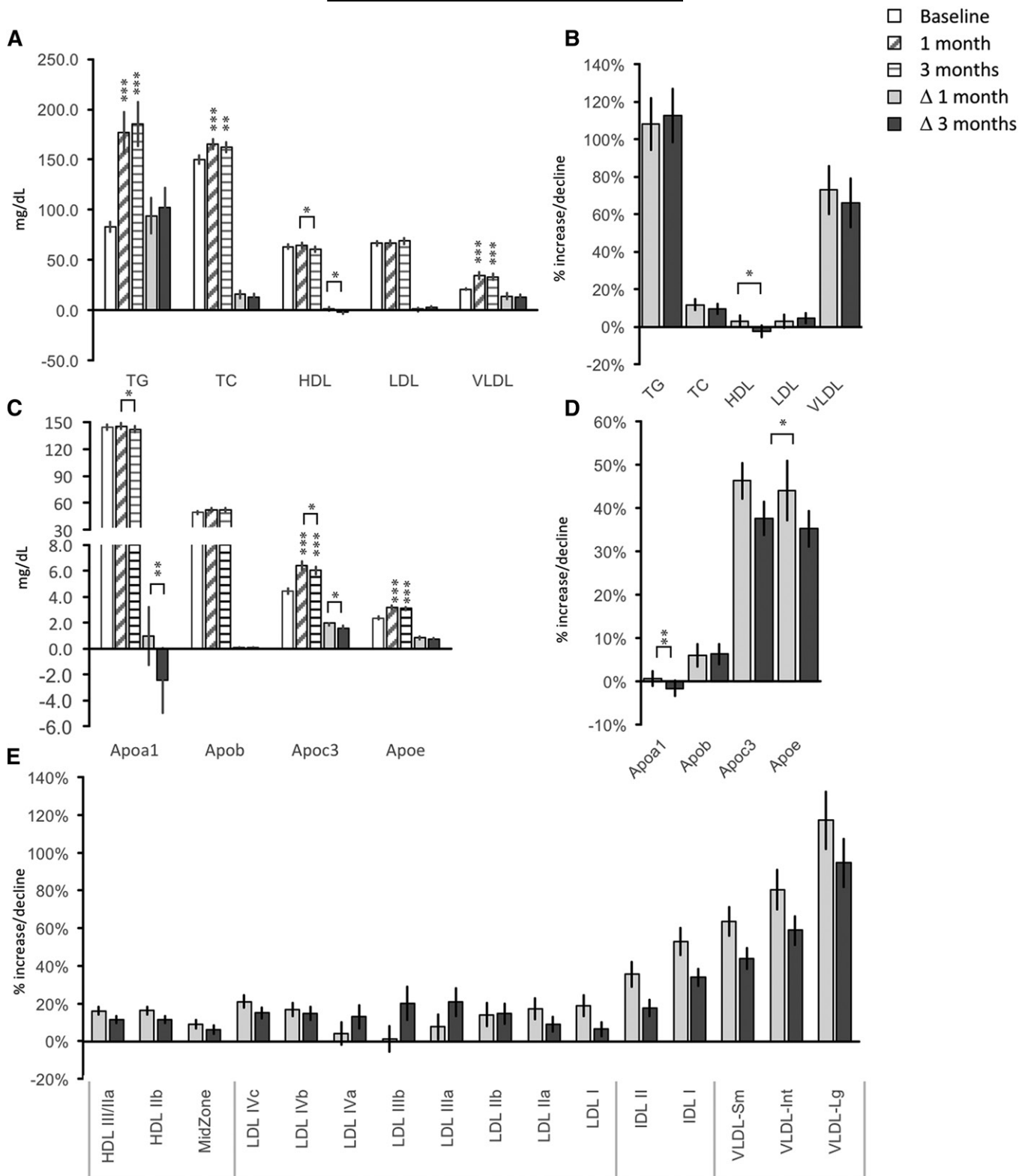
Fig. 1. Impact of dietary supplementation with fructose on lipid profiles. A: Fasting concentrations of TG, TC, HDL-C, LDL-C, and VLDL-C. B: Percent increase above baseline after 1 and 3 months of fructose consumption for the measures shown in panel A. C: Fasting concentrations of apolipoproteins. D: Percent increase above baseline after 1 and 3 months of fructose consumption for the measures shown in panel B. E: Percent increase above baseline after 1 and 3 months of fructose consumption for lipoproteins subfractionated by particle diameter. Significant differences are indicated by asterisks: significant differences of 1 and 3 month values from baseline, or by lines between specific time points, are indicated; ***$P < 0.001$; **$P < 0.01$; *$P < 0.05$. Statistics for actual values for the data in E are provided in Table 2.

TABLE 2. Impact of dietary supplementation with fructose on plasma concentrations (nmol/L) of lipoprotein fractionated by particle diameter

	Prefructose Measurement	1 Month Fructose Measurement (Change in Conc.)	3 Months Fructose Measurement (Change in Conc.)	Diet Effect
HDL III and IIa	$16,774 \pm 258$	$19,360 \pm 355^a$ $(2,586 \pm 330)$	$18,597 \pm 316^a$ $(1,823 \pm 299)$	$P < 0.001$
HDL IIb	$8,610 \pm 223$	$9,359 \pm 239^b$ (748 ± 223)	$8,980 \pm 257^b$ (370 ± 226)	$P < 0.05$
MidZone	966 ± 21	$1,046 \pm 27^a$ (79 ± 21)	$1,013 \pm 24$ (44 ± 24)	$P < 0.005$
LDL IVc	68 ± 2	82 ± 3^a (14 ± 2)	77 ± 2^a (9 ± 2)	$P < 0.001$
LDL IVb	44 ± 1	51 ± 2^a (6 ± 1)	50 ± 2^a (6 ± 2)	$P < 0.001$
LDL IVa	44 ± 2	42 ± 2 (-1 ± 2)	48 ± 3 (4 ± 3)	n.s.
LDL IIIb	38 ± 2	36 ± 3 (-2 ± 2)	43 ± 3^e (5 ± 3)	$P < 0.05$
LDL IIIa	86 ± 4	88 ± 6 (2 ± 6)	100 ± 7^d (14 ± 6)	$P < 0.05$
LDL IIb	88 ± 4	94 ± 5 (6 ± 5)	97 ± 5 (9 ± 5)	n.s.
LDL IIa	75 ± 3	83 ± 3 (8 ± 4)	79 ± 3 (4 ± 3)	$P < 0.05$
LDL I	113 ± 4	128 ± 5^e (16 ± 5)	117 ± 5 (5 ± 4)	$P < 0.05$
IDL II	107 ± 5^f	139 ± 6^f (31 ± 6)	121 ± 5^f (14 ± 4)	$P < 0.001$
IDL I	82 ± 4^f	121 ± 7^f (39 ± 6)	107 ± 5^f (25 ± 4)	$P < 0.001$
VLDL-Sm	27 ± 1^f	43 ± 3^f (16 ± 2)	38 ± 2^f (11 ± 1)	$P < 0.001$
VLDL-Int	19 ± 1^g	34 ± 3^g (15 ± 3)	30 ± 3^g (11 ± 2)	$P < 0.001$
VLDL-Lg	8 ± 1	17 ± 2^a (9 ± 2)	15 ± 2^a (7 ± 1)	$P < 0.001$

In the third and fourth columns, changes in concentration (Conc.) are in parentheses. n.s., not significant.

[a] $P < 0.001$, significantly different from prefructose.

[b] $P < 0.01$, significantly different from prefructose.

[c] $P < 0.001$, significantly different from 1 month fructose.

[d] $P < 0.05$ versus prefructose, $P < 0.01$ versus 1 month; significantly different from prefructose and 1 month fructose.

[e] $P < 0.01$ versus prefructose, $P < 0.05$ versus 3 months; significantly different from prefructose and 3 months fructose.

[f] $P < 0.01$; values significantly different at all times measured.

[g] $P < 0.001$ (prefructose vs. 3 months), $P < 0.05$ (1 month vs. 3 months); values significantly different at all times measured.

baseline conditions also correlated with fructose-induced increases of fasting plasma TG concentrations in the model. The independent variables were baseline (prefructose) and Δs for body weight, glucose, insulin, HOMA-IR, leptin, adiponectin, ApoC3, and ApoE.

For increases of fasting plasma TG, the selected variables explained 62.3% of the variation after 1 month and 51.6% after 3 months of fructose consumption (**Table 3**) ($R^2 = 0.62$ after 1 month, $P < 0.001$; $R^2 = 0.52$ after 3 months, $P = 0.004$). Increases in plasma concentrations of ApoC3, but not ApoE, exhibited a strong association with increases in TG at both time points in the model (**Fig. 3A**, B). Modeling for fructose-induced increases of fasting plasma total IDL or VLDL particles in animals fed fructose was less successful and not consistent at the 1 and 3 month time points. Modeling for changes in VLDL particles after 1 month of fructose explained 50% of the variability ($R^2 = 0.501$, $P < 0.01$); ΔApoC3 and Δadiponectin are significant variables in the model ($P = 0.001$ for ΔApoC3, $P < 0.05$ for Δadiponectin). Modeling was successful in partially calculating increases of IDL particles after 1 month of fructose consumption ($R^2 = 0.471$, $P < 0.05$).

ApoC3 RNAi reverses fructose-induced hypertriglyceridemia

An RNAi-based strategy was used to investigate whether reduction of circulating ApoC3 by inhibiting ApoC3 expression with an RNAi trigger targeting *APOC3* mRNA (ARO-APOC3) would reduce hypertriglyceridemia resulting from consumption of a high-sugar (HFCS) diet. Animals provided two 500 ml beverages containing HFCS (15% by weight) and consuming a moderate fat diet (see the Materials and Methods) rapidly developed elevated

fasting plasma ApoC3 concentrations and fasting hypertriglyceridemia (**Fig. 4**). Fasting TG concentrations increased by more than 3-fold, from 87 ± 23 mg/dl to 316 ± 91 mg/dl ($\Delta = +177 \pm 80$ mg/dl; $P < 0.05$, n = 6). Nonfasting TG concentrations also increased from 158 ± 38 mg/dl to 523 ± 196 mg/dl ($\Delta = +365 \pm 163$ mg/dl; $P < 0.05$). Fasting ApoC3 concentrations increased by ~50%, from 5.9 ± 0.3 mg/dl to 8.8 ± 1.9 mg/dl (n = 6).

In the four animals treated with injections of ARO-APOC3, there was a rapid decline in fasting plasma ApoC3 concentrations from 10.0 ± 2.8 mg/dl to 3.2 ± 0.5 mg/dl ($\Delta = -6.8 \pm 2.4$ mg/dl; $P < 0.025$) during days 43–85 after the first injection of ARO-APOC3 (Fig. 4A), with levels falling by $-65 \pm 4\%$ from pretreatment levels ($P < 0.001$, days 43–85 vs. "baseline" pretreatment values at day 8) (Fig. 4B). Fasting TG concentrations declined significantly during days 43–85 following the first injection from 310 ± 140 mg/dl to 118 ± 38 mg/dl (%$\Delta = -48.5 \pm 13.0\%$; $P < 0.025$) and nonfasting TG concentrations decreased from 620 ± 293 mg/dl to 220 ± 71 mg/dl (%$\Delta = -55.7 \pm 9.0$; $P < 0.005$) at days 56 and 84 posttreatment. The decreases of TG levels were most pronounced in animals with the most marked degree of pretreatment hypertriglyceridemia (Fig. 4C, D). In the other two animals on the moderate fat plus HFCS diet that were treated with vehicle, fasting ApoC3, fasting TG, and nonfasting TG concentrations were unchanged from baseline pretreatment levels (data not shown).

FO supplementation produces a rapid and sustained shift of lipoprotein particle distribution away from IDL and VLDL

Supplementation with FO (4 g/day) attenuates the fructose-induced increases of both TG and ApoC3 concentrations
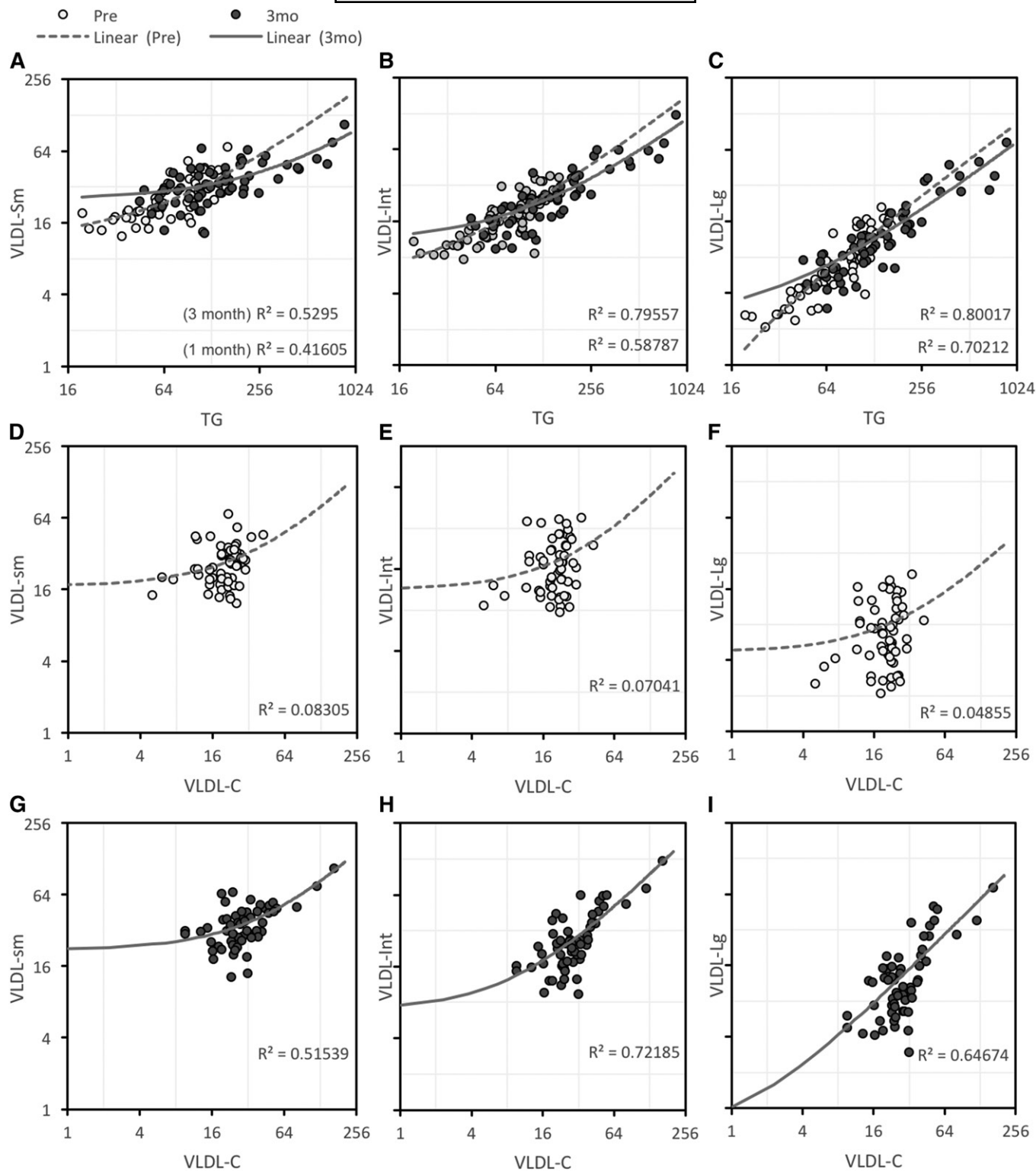
Fig. 2. Relationships between TG, VLDL-C, and VLDL subfractions at baseline (chow-fed) and after 3 months of fructose consumption. A–C: Relationships between TG and small (A), intermediate (B), and large (C) VLDL subfractions. D–F: Weak relationships between VLDL-C and small (D), intermediate (E), and large (F) VLDL subfractions at baseline. Relationships between VLDL-C and VLDL subfractions is stronger after 3 months of fructose consumption. G–I: VLDL-C and small (G), intermediate (H), and large (I) subfractions. Units for TG and VLDL-C are milligrams per deciliter, subfractions are nanomoles per liter.

(22). In the current study, we also observed that FO reversed the marked fructose-induced shift of lipoprotein particle size toward IDL and VLDL (**Fig. 5A**, B). While fructose consumption nearly doubled the concentration of large VLDL particles ($\%\Delta = 95.4 \pm 35.6\%$; $P < 0.03$) in nine control animals after 6 months on the high-fructose diet, VLDL-Lg actually decreased significantly in the 10 animals that received FO ($\%\Delta = -25.4 \pm 7.4$; $P < 0.005$ vs. control),

TABLE 3. Multivariate linear regression results for predictors of fructose-induced changes (Δ) in fasting plasma concentrations of TG

Dependent Variable:	Δ TG	
Variables entered:	1 Month Fructose	3 Months Fructose
Apoc3 (baseline)	0.671	0.536
ΔApoc3	**<0.001**	**0.002**
Apoe (baseline)	0.866	0.429
ΔApoE	0.820	0.343
Insulin (baseline)	0.419	0.463
ΔInsulin	0.316	**0.029**
Glucose (baseline)	0.445	0.457
ΔGlucose	0.283	**0.022**
HOMA-IR (baseline)	0.422	0.466
ΔHOMA-IR	0.330	**0.030**
Leptin (baseline)	**0.001**	0.771
ΔLeptin	**0.009**	0.076
Body weight (baseline)	0.586	0.604
ΔBody weight	0.541	0.995
Adiponectin (baseline)	0.380	0.738
ΔAdiponectin	0.085	0.518

Significant values are in bold text. Modeling explained 62% of the variability in fructose-induced increase in TG after 1 month (R2 = 0.623, $P < 0.001$) and 52% after 3 months ($R^2 = 0.516$, $P = 0.004$).

despite sustained consumption of fructose. Similar results were also observed earlier at the 1 and 3 month time points in the monkeys consuming fructose along with FO compared with those consuming fructose alone (Fig. 5C–E). The lipoprotein particle distribution in the fructose-fed animals supplemented with FO was shifted from IDL and VLDL primarily to intermediate-sized LDL particles.

The effect of FO supplementation was further assessed in liver biopsies obtained from a separate group of rhesus macaques (n = 4/group). Analysis of liver gene expression by RNA-seq indicated significant changes of hepatic gene expression in animals fed the moderate-fat diet plus HFCS-sweetened beverages plus FO, as opposed to the HFCS diet with the blended soybean and canola control oil (see the supplemental data). Using $P < 0.05$ as the selection criteria, 269 upregulated and 307 downregulated transcripts were identified. Pathway analysis of genes that were downregulated identified "activation of gene expression by SREBF (SREBP)" and "regulation of cholesterol synthesis by SREBP (SREBF)" as being highly significant (P value 6.81 × 10^{-10}, $3.81 × 10^{-8}$) (**Table 4**). This group of genes included enzymes involved in fatty acid synthesis [e.g., ACACA and FASN], as well as genes critical for cholesterol synthesis (HMGCR) and lipoprotein metabolism [PCSK9, LDL receptor (LDLR)]. The effects of FO supplementation on the expression of ACACA, encoding ACACA α that catalyzes the carboxylation of acetyl-CoA to malonyl-CoA (the rate-limiting step in de novo lipogenesis), and the gene that was most significantly downregulated in the RNA-seq analysis were confirmed using qRT-PCR in a larger cohort (∼2-fold, $P = 0.006$, n = 7) (**Fig. 6**).

DISCUSSION

The results from this study provide further evidence of a strong correlation between plasma ApoC3 concentrations and fructose-induced elevations of circulating TG-rich VLDL-C. They also further support the use of the fructose-fed rhesus macaque as a relevant nonhuman primate model of diet-induced MetS, and in particular the dyslipidemic and
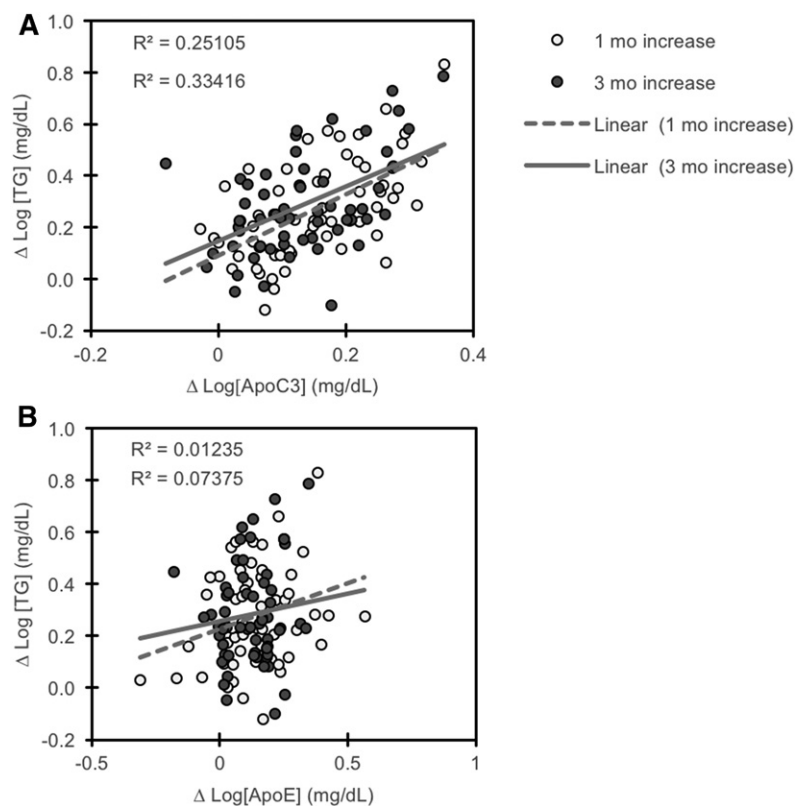

Fig. 3. Increases in plasma concentrations of TG with fructose consumption are correlated with increases of ApoC3 (A) but not ApoE (B). Data are log-transformed.
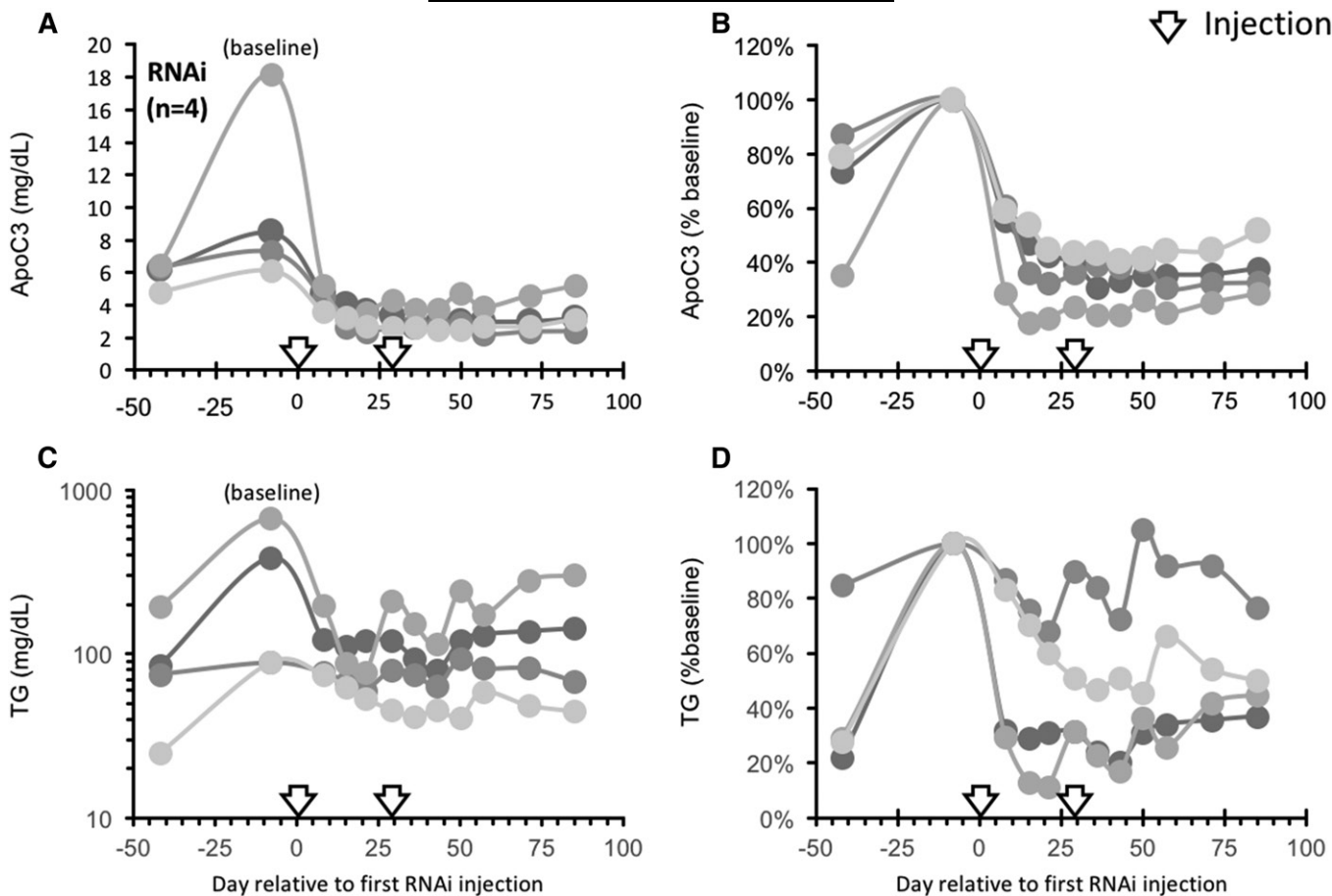
Fig. 4. Suppression of ApoC3 using RNAi reverses hypertriglyceridemia induced by HFCS. Adult male rhesus macaques (n = 4) were provided 500 ml of a HFCS beverage (15% by weight) twice daily. Fasting plasma samples were collected at the times indicated and assayed for ApoC3 (A, B) or TG (C, D). Data shown are actual values (A, C) or percent baseline (34 days of HFCS). After 42 days, the animals received a single subcutaneous injection of ApoC3-RNAi (4 mg/kg) on study days 0 and 29 (indicated by arrows).

insulin resistance components of MetS (18–20). Rhesus macaques that are provided fructose as a flavored beverage rapidly enter a state of positive energy balance and exhibit symptoms of MetS. Large increases of fasting plasma insulin and TG concentrations are observed after only 1 month of fructose consumption.

Recent studies in mouse models suggest that the small intestine is a major site of fructose disposal, where it is converted to glucose, lactate, glycerate, and organic acids (26). However, the intestine appears to have an upper limit for metabolizing fructose, with higher doses resulting in significant levels of fructose accumulating in the liver or metabolized by colonic microbiota. In the liver, fructose increases de novo lipogenesis as it bypasses a key regulatory point in glycolysis (27). The results from the current study are consistent with fructose consumption increasing circulating levels of large TG-rich VLDL particles in rhesus macaques. Increased rates of de novo lipogenesis are likely to contribute to this effect (27, 28); although the increases of ApoC3 suggest that reduced clearance of TG-rich remnant lipoproteins may also contribute.

A strong association between fasting plasma VLDL-C concentrations with VLDL-Lg, and with TG, suggests that large VLDL particles are enriched with both TG and cholesterol

esters. In humans, supplementing the diet with fructose beverages has a dose-dependent effect to modestly but significantly increase LDL-C (28–30). In the current study, fructose consumption was associated with a modest (~10%) increase of TC, but no significant change in LDL-C levels. While there was a significant change in HDL-C concentrations, the magnitude of the effect was very small (<5%) and not consistent between the 1 and 3 month time points. While plasma concentrations of total LDL-C did not increase during fructose consumption, there were significant increases of small dense LDL particles measured using ion mobility. The discrepancy between the two measurements is suggestive of accumulation of TG in lipoprotein remnant particles.

It is also worth noting that, while ApoA1 and ApoB concentrations did not exhibit major increases in the group as a whole, ΔApoA1 and ΔApoB correlated with fructose-induced changes in TC levels in individual animals (ΔApoB, $P < 0.001$; ΔApoA1, $P < 0.05$). Strong correlations were also observed between ΔApoB and ΔLDL-C ($P = 0.001$). The current study focused on the changes in plasma TG concentration with fructose consumption, with the majority (56/59) of animals exhibiting increases of plasma TG concentrations during 3 months of fructose consumption. There was significant variation between animals in how
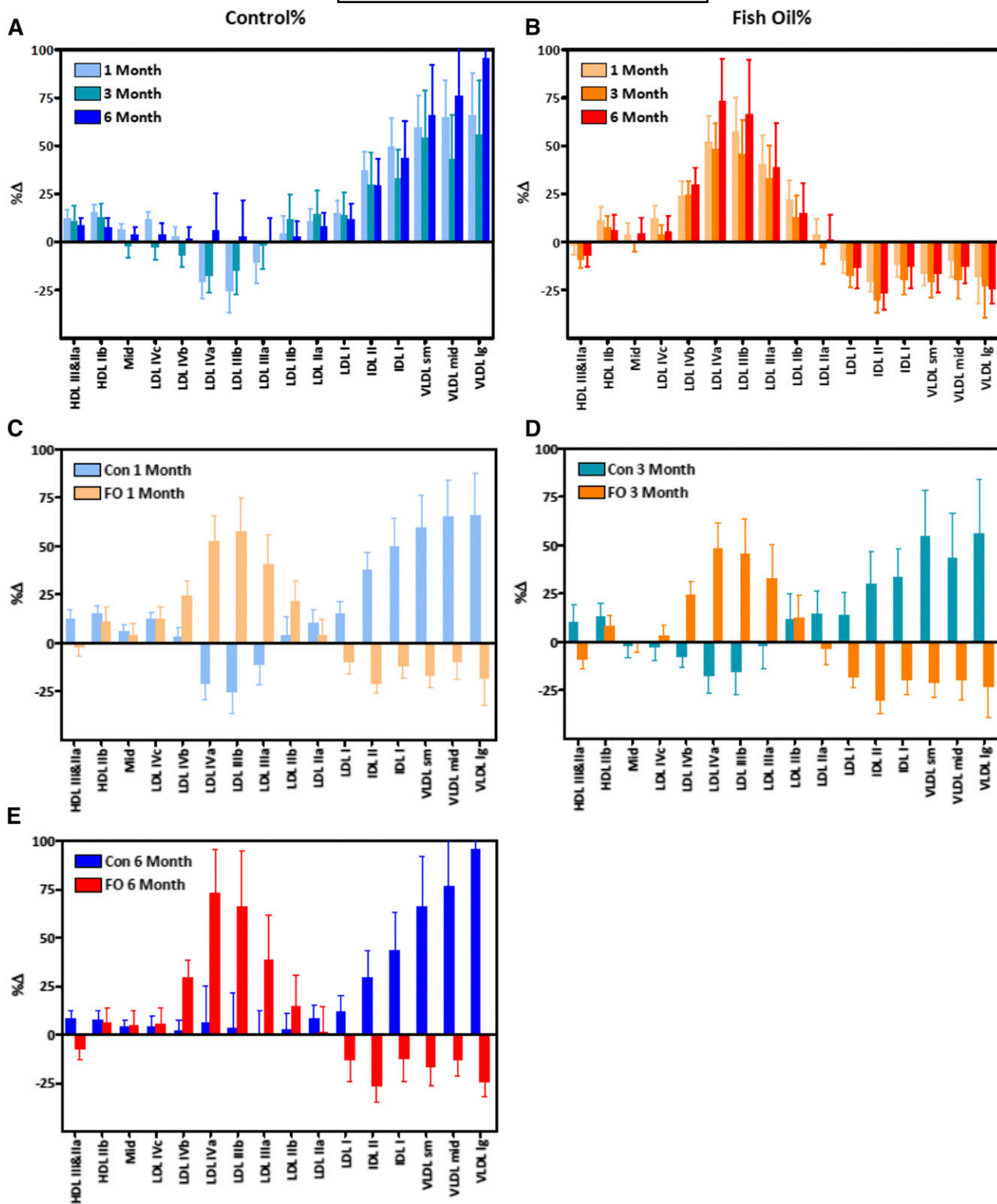
Fig. 5. A FO dietary supplement alters the effects of fructose on the distribution of lipoprotein particles. A: Increases in lipoprotein particles in rhesus macaques provided fructose (n = 9). The data shown are percent increases above baseline (chow-fed) condition (%Δ). B: Increases in lipoprotein particles in rhesus macaques provided fructose and FO (n = 10). In panels C–E, %Δs are compared between fructose only (Con) and fructose+FO (FO) groups after 1 month (C), 3 months (D), or 6 months (E).

fructose consumption affects cholesterol metabolism. This variation may be explained by genetic differences between animals resulting in the differences in differential expression of genes regulating cholesterol homeostasis.

A significant finding of this study is the observation that increases of circulating ApoC3 concentrations correlate consistently with fructose-induced hypertriglyceridemia. While insulin resistance is often associated with dyslipidemia,

TABLE 4. FO supplementation alters hepatic expression of genes involved in lipid metabolism.

Gene Symbol	Fold Change [(HFCS+FO)/HFCS]	1/(Fold Change)	P	P (Adjusted)
Transcription factors				
SREBF1	0.72	1.39	0.035	1.000
SREBF2	0.72	1.38	0.031	1.000
Fatty acid synthesis/metabolism				
ACACA	0.50	1.98	1.35E-07	3.47E-04
ACOT12	0.71	1.40	0.004	0.811
ACSF3	0.67	1.50	0.001	0.446
ACSL3	0.69	1.45	0.011	1.000
ACSS2	0.71	1.40	0.036	1.000
ELOVL5	0.74	1.35	0.022	1.000
FABP4	0.62	1.61	0.000	0.238
FADS1	0.60	1.68	0.001	0.475
FADS2	0.74	1.36	0.018	1.000
FASN	0.65	1.53	0.007	0.972
Cholesterol synthesis/metabolism				
ABCG8	0.79	1.26	0.033	1.000
DHCR7	0.69	1.45	0.021	1.000
FDFT1	0.67	1.49	0.001	0.304
FDPS	0.54	1.85	0.000	0.033
HMGCR	0.66	1.51	0.006	0.932
HMGCS1	0.57	1.76	0.000	0.238
IDI1	0.65	1.55	0.006	0.931
LSS	0.68	1.46	0.017	1.000
MVD	0.66	1.51	0.009	0.997
SC5D	0.73	1.37	0.027	1.000
Lipoprotein metabolism				
PCSK9	0.64	1.57	0.005	0.895
LDLR	0.70	1.42	0.026	1.000
LRP4	0.72	1.40	0.037	1.000
APOC2	0.72	1.38	0.033	1.000
APOL3	1.47	0.68	0.010	1.000
APOL4	1.49	0.67	0.012	1.000
CYP enzymes				
CYP1B1	0.46	2.16	0.000	0.001
CYP21A2	0.62	1.62	0.001	0.446
CYP2B6	0.75	1.33	0.030	1.000
CYP51A1	0.53	1.90	0.000	0.062

Data are expressed as fold change in animals fed HFCS and FO (HFCS+FO) relative to animals provided the HFCS and control oil.

indices of insulin resistance (insulin, HOMA-IR) did not exhibit strong associations with fructose-induced increases in fasting plasma concentrations of TG and large TG-rich VLDL-C in modeling using linear regression.

There is evidence in humans that ApoC3 expression is a significant contributor to risk for CVD (7–9), while loss-of-function mutations of ApoC3 are protective against the development of CVD (5). In the current study, fructose
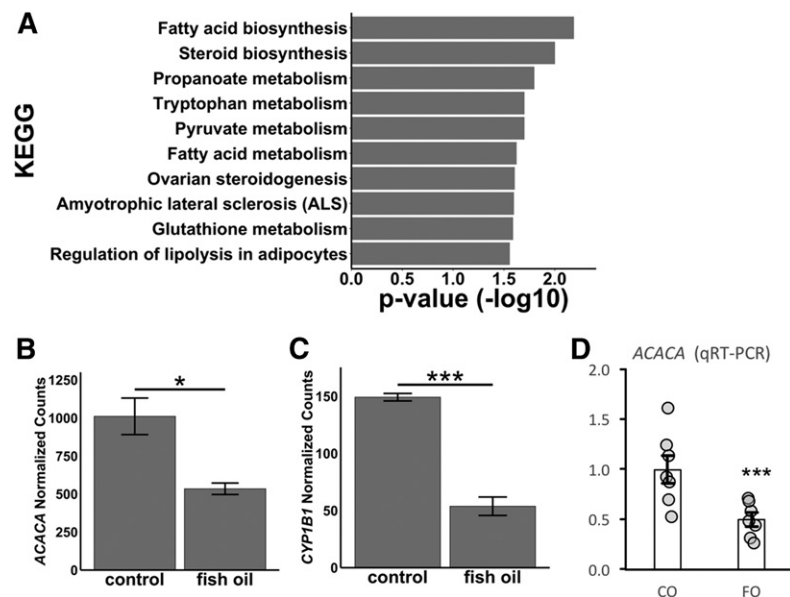

Fig. 6. A FO dietary supplement significantly reduces liver ACACA expression. A: KEGG pathway enrichment analysis for hepatic genes significantly (adjusted $P < 0.05$) downregulated by FO compared with control (sunflower oil). B: ACACA expression (DESeq2 normalized counts) by RNA-seq analysis in control and FO treatment conditions (n = 4/group). C: CYP1B1 expression (DESeq2 normalized counts) by RNA-seq analysis in control and FO treatment conditions (n = 4/group). D: Validation of the *ACACA* expression by qRT-PCR in control and FO (n = 7/group). Error bars represent SEM. *$P < 0.05$; ***$P < 0.01$.

consumption rapidly (within 1 month) increases fasting plasma ApoC3 concentrations. Plasma ApoC3 concentrations also increase dose-dependently after only 2 weeks of consuming dietary sugar (HFCS) in humans (29). The relationship between plasma total and lipoprotein cholesterol and risk for CVD in rhesus macaques has not been well studied. However, atherosclerosis has been observed in rhesus macaques fed high-fat diets (31). However, it is important to note that similar changes in ApoC3 and TG have been associated with decreased or increased risk for CVD in humans (5, 7–9).

Fructose-induced changes of ApoE and ApoC3 concentrations were highly correlated. The C-terminal region of ApoE contributes to the regulation of TG-rich lipoprotein clearance by functioning as a LDLR-binding site (32). ApoC3 affects the uptake of TG-rich lipoproteins by the LDLR and LDLR-related protein 1 (LRP1) (33). However, increases in ApoC3 but not ApoE were strongly associated with fructose-induced hypertriglyceridemia. The significance of this observation is unclear but suggests that of the two apolipoproteins, the functions of ApoC3 are the predominant variable driving changes in circulating TG concentrations. We were also able to demonstrate that suppression of ApoC3 synthesis, using RNAi methodology, reversed hypertriglyceridemia in animals maintained on a moderate-fat diet and consuming HFCS-sweetened beverages two times a day. These initial data from n = 4 animals suggest a mechanistic link between circulating ApoC3 and TG concentrations because specific reductions of ApoC3 with RNAi lead to an amelioration of fasting hypertriglyceridemia resulting from the consumption of a high-sugar diet. Postprandial TGs were also measured in the RNAi experiment, and exhibited similar responses to ARO-APOC3.

The mechanisms linking ApoC3 to adverse effects on lipid metabolism remain controversial. Results from early studies in ApoC3 transgenic mice suggested reduced cellular uptake of TG-rich particles (11). Additional studies indicated that ApoC3 inhibits LPL (34–37); at higher concentrations, ApoC3 also appears to inhibit hepatic lipase (38). Reductions of TG observed with volanesorsen treatment are independent of effects on LPL (12). A hypothesis is that ApoC3 increases TG levels by affecting uptake of TG-rich lipoproteins by the LDLR and LRP1 (33).

The effects of FO supplementation on changes of lipoprotein particle size distribution in fructose-fed rhesus monkeys are novel and interesting. We have previously reported that FO provided at a dose of 4 g/day largely prevents the increases of both plasma ApoC3 and circulating TG concentrations in the fructose-fed rhesus monkey model of MetS (20), and EPA+DHA together have been shown to lower circulating ApoC3 in humans (39). It is likely that these effects are related, based on the strong associations between plasma concentrations of ApoC3 and TG in response to fructose feeding.

A previous study using rhesus macaques examined the effects of FO on lipid metabolism and dyslipidemia induced by a diet supplemented with saturated fat and cholesterol (2% cholesterol, 25% coconut oil) (40). In that study, FO reduced the number of VLDL, IDL, and LDL particles in plasma, and reduced cholesterol ester content of lipoproteins. In the current study, the impact of FO of fructose-induced hypertriglyceridemia appears to involve suppression of hepatic lipogenic enzymes. RNA-seq analysis suggests that FO supplementation reduces the activity of the SREBPF family of transcription factors known to drive expression of enzymes involved in fatty acid and cholesterol synthesis and metabolism, particularly ACACA (41). These findings are generally consistent with results from experiments examining the impact of FO on hepatic gene expression in mice (42) and in primary cultured rat hepatocytes (43). Reduced de novo lipogenesis is a plausible explanation for the reduction of VLDL-C levels observed in fructose-fed animals provided the FO dietary supplement. Inhibition of SREBF2-mediated transcription of the *LDLR* gene also provides a plausible explanation (reduced LDLR-mediated clearance) for the accumulation of LDL-particles observed with FO treatment. FO supplementation also reduced the expression of cytochrome P450 (CYP)1B1. This member of the CYP superfamily is known to be important for regulating steroid and fatty acid metabolism, and has been suggested to be a potential target for the treatment of the metabolic diseases of obesity (44).

There are several mechanisms by which FO, and the omega-3 and furan fatty acids it contains, may produce lowering of TG concentrations and the shift away from large TG-rich lipoproteins. First, FO has been demonstrated to inhibit de novo lipogenesis in human subjects during overfeeding of a high-fructose diet, and our gene expression data (e.g., reduced ACACA expression) support this conclusion. (45). This response may be mediated in part by the actions of omega-3 fatty acids (EPA and DHA) to downregulate genes involved in hepatic lipid biosynthesis, including FASN (46). In addition, the actions of FO to prevent the fructose diet-induced increase of ApoC3 (20) may contribute to its effects to prevent and even reduce the increases of larger IDL and VLDL particles while increasing the amount of smaller-sized LDL particles. This mechanism would involve generating smaller-sized LDL particles via increased hydrolysis of TG from larger TG-rich VLDL and IDL particles due to enhanced lipase activity that is unrestrained by ApoC3.

In summary, the results from the present study provide a further compelling link between excess consumption of beverages sweetened with fructose-containing sugars and dyslipidemia as well as new information on the potential protective effects of FO and omega-3 fatty acids. They also support the use of the fructose- and HFCS-fed rhesus macaques as a nonhuman primate model for preclinical studies evaluating novel therapies targeting dyslipidemia in general and ApoC3 in particular.

REFERENCES

1. Navarese, E. P., J. G. Robinson, M. Kowalewski, M. Kolodziejczak, F. Andreotti, K. Bliden, U. Tantry, J. Kubica, P. Raggi, and P. A. Gurbel. 2018. Association between baseline LDL-C level and total and cardiovascular mortality after LDL-C lowering: a systematic review and meta-analysis. *JAMA.* **319:** 1566–1579.

2. Siri-Tarino, P. W., and R. M. Krauss. 2016. The early years of lipoprotein research: from discovery to clinical application. *J. Lipid Res.* **57:** 1771–1777.

3. Sathiyakumar, V., K. Kapoor, S. R. Jones, M. Banach, S. S. Martin, and P. P. Toth. 2018. Novel therapeutic targets for managing dyslipidemia. *Trends Pharmacol. Sci.* **39:** 733–747.

4. Nordestgaard, B. G., S. J. Nicholls, A. Langsted, K. K. Ray, and A. Tybjaerg-Hansen. 2018. Advances in lipid-lowering therapy through gene-silencing technologies. *Nat. Rev. Cardiol.* **15:** 261–272.

5. Khetarpal, S. A., A. Qamar, J. S. Millar, and D. J. Rader. 2016. Targeting ApoC-III to Reduce Coronary Disease Risk. *Curr. Atheroscler. Rep.* **18:** 54.

6. Ramms, B., and P. Gordts. 2018. Apolipoprotein C-III in triglyceride-rich lipoprotein metabolism. *Curr. Opin. Lipidol.* **29:** 171–179.

7. Pollin, T. I., C. M. Damcott, H. Shen, S. H. Ott, J. Shelton, R. B. Horenstein, W. Post, J. C. McLenithan, L. F. Bielak, P. A. Peyser, et al. 2008. A null mutation in human APOC3 confers a favorable plasma lipid profile and apparent cardioprotection. *Science.* **322:** 1702–1705.

8. Jørgensen, A. B., R. Frikke-Schmidt, B. G. Nordestgaard, and A. Tybjaerg-Hansen. 2014. Loss-of-function mutations in APOC3 and risk of ischemic vascular disease. *N. Engl. J. Med.* **371:** 32–41.

9. TG and HDL Working Group of the Exome Sequencing Project, National Heart, Lung, and Blood Institute, J. Crosby, G. M. Peloso, P. L. Auer, D. R. Crosslin, N. O. Stitziel, L. A. Lange, Y. Lu, Z. Z. Tang, H. Zhang, et al. 2014. Loss-of-function mutations in APOC3, triglycerides, and coronary disease. *N. Engl. J. Med.* **371:** 22–31.

10. Ito, Y., N. Azrolan, A. O'Connell, A. Walsh, and J. L. Breslow. 1990. Hypertriglyceridemia as a result of human apo CIII gene expression in transgenic mice. *Science.* **249:** 790–793.

11. Aalto-Setälä, K., E. A. Fisher, X. Chen, T. Chajek-Shaul, T. Hayek, R. Zechner, A. Walsh, R. Ramakrishnan, H. N. Ginsberg, and J. L. Breslow. 1992. Mechanism of hypertriglyceridemia in human apolipoprotein (apo) CIII transgenic mice. Diminished very low density lipoprotein fractional catabolic rate associated with increased apo CIII and reduced apo E on the particles. *J. Clin. Invest.* **90:** 1889–1900.

12. Gaudet, D., V. J. Alexander, B. F. Baker, D. Brisson, K. Tremblay, W. Singleton, R. S. Geary, S. G. Hughes, N. J. Viney, M. J. Graham, et al. 2015. Antisense inhibition of apolipoprotein C-III in patients with hypertriglyceridemia. *N. Engl. J. Med.* **373:** 438–447.

13. Yang, X., S. R. Lee, Y. S. Choi, V. J. Alexander, A. Digenio, Q. Yang, Y. I. Miller, J. L. Witztum, and S. Tsimikas. 2016. Reduction in lipoprotein-associated apoC-III levels following volanesorsen therapy: phase 2 randomized trial results. *J. Lipid Res.* **57:** 706–713.

14. Rimm, E. B., L. J. Appel, S. E. Chiuve, L. Djousse, M. B. Engler, P. M. Kris-Etherton, D. Mozaffarian, D. S. Siscovick, and A. H. Lichtenstein; American Heart Association Nutrition Committee of the Council on Lifestyle and Cardiometabolic Health; Council on Epidemiology and Prevention; and Council on Clinical Cardiology. 2018. Seafood long-chain n-3 polyunsaturated fatty acids and cardiovascular disease: a science advisory from the American Heart Association. *Circulation.* **138:** e35–e47.

15. Siscovick, D. S., T. A. Barringer, A. M. Fretts, J. H. Wu, A. H. Lichtenstein, R. B. Costello, P. M. Kris-Etherton, T. A. Jacobson, M. B. Engler, H. M. Alger, et al; American Heart Association Nutrition Committee of the Council on Lifestyle and Cardiometabolic Health; Council on Epidemiology and Prevention; Council on Cardiovascular Disease in the Young; Council on Cardiovascular and Stroke Nursing; and Council on Clinical Cardiology. 2017. Omega-3 polyunsaturated fatty acid (fish oil) supplementation and the prevention of clinical cardiovascular disease: a science advisory from the American Heart Association. *Circulation.* **135:** e867–e884.

16. Shearer, G. C., O. V. Savinova, and W. S. Harris. 2012. Fish oil–how does it reduce plasma triglycerides? *Biochim. Biophys. Acta.* **1821:** 843–851.

17. Bremer, A. A., K. L. Stanhope, J. L. Graham, B. P. Cummings, W. Wang, B. R. Saville, and P. J. Havel. 2011. Fructose-fed rhesus monkeys: a nonhuman primate model of insulin resistance, metabolic syndrome, and type 2 diabetes. *Clin. Transl. Sci.* **4:** 243–252.

18. Kleinert, M., C. Clemmensen, S. M. Hofmann, M. C. Moore, S. Renner, S. C. Woods, P. Huypens, J. Beckers, M. H. de Angelis, A. Schurmann, et al. 2018. Animal models of obesity and diabetes mellitus. *Nat. Rev. Endocrinol.* **14:** 140–162.

19. Havel, P. J., P. Kievit, A. G. Comuzzie, and A. A. Bremer. 2017. Use and importance of nonhuman primates in metabolic disease research: current state of the field. *ILAR J.* **58:** 251–268.

20. Bremer, A. A., K. L. Stanhope, J. L. Graham, B. P. Cummings, S. B. Ampah, B. R. Saville, and P. J. Havel. 2014. Fish oil supplementation ameliorates fructose-induced hypertriglyceridemia and insulin resistance in adult male rhesus macaques. *J. Nutr.* **144:** 5–11.

21. Robbins, M., A. Judge, and I. MacLachlan. 2009. siRNA and innate immunity. *Oligonucleotides.* **19:** 89–102.

22. Caulfield, M. P., S. Li, G. Lee, P. J. Blanche, W. A. Salameh, W. H. Benner, R. E. Reitz, and R. M. Krauss. 2008. Direct determination of lipoprotein particle sizes and concentrations by ion mobility analysis. *Clin. Chem.* **54:** 1307–1316.

23. Mora, S., M. P. Caulfield, J. Wohlgemuth, Z. Chen, H. R. Superko, C. M. Rowland, R. J. Glynn, P. M. Ridker, and R. M. Krauss. 2015. Atherogenic lipoprotein subfractions determined by ion mobility and first cardiovascular events after random allocation to high-intensity statin or placebo: the Justification for the Use of Statins in Prevention: an Intervention Trial Evaluating Rosuvastatin (JUPITER) Trial. *Circulation.* **132:** 2220–2229.

24. Stern, J. H., J. M. Rutkowski, and P. E. Scherer. 2016. Adiponectin, leptin, and fatty acids in the maintenance of metabolic homeostasis through adipose tissue crosstalk. *Cell Metab.* **23:** 770–784.

25. Vergès, B. 2015. Pathophysiology of diabetic dyslipidaemia: where are we? *Diabetologia.* **58:** 886–899.

26. Jang, C., S. Hui, W. Lu, A. J. Cowan, R. J. Morscher, G. Lee, W. Liu, G. J. Tesz, M. J. Birnbaum, and J. D. Rabinowitz. 2018. The small intestine converts dietary fructose into glucose and organic acids. *Cell Metab.* **27:** 351–361.e3.

27. Havel, P. J. 2005. Dietary fructose: implications for dysregulation of energy homeostasis and lipid/carbohydrate metabolism. *Nutr. Rev.* **63:** 133–157.

28. Stanhope, K. L., J. M. Schwarz, N. L. Keim, S. C. Griffen, A. A. Bremer, J. L. Graham, B. Hatcher, C. L. Cox, A. Dyachenko, W. Zhang, et al. 2009. Consuming fructose-sweetened, not glucose-sweetened, beverages increases visceral adiposity and lipids and decreases insulin sensitivity in overweight/obese humans. *J. Clin. Invest.* **119:** 1322–1334.

29. Stanhope, K. L., V. Medici, A. A. Bremer, V. Lee, H. D. Lam, M. V. Nunez, G. X. Chen, N. L. Keim, and P. J. Havel. 2015. A dose-response study of consuming high-fructose corn syrup-sweetened beverages on lipid/lipoprotein risk factors for cardiovascular disease in young adults. *Am. J. Clin. Nutr.* **101:** 1144–1154.

30. Stanhope, K. L., A. A. Bremer, V. Medici, K. Nakajima, Y. Ito, T. Nakano, G. Chen, T. H. Fong, V. Lee, R. I. Menorca, et al. 2011. Consumption of fructose and high fructose corn syrup increase postprandial triglycerides, LDL-cholesterol, and apolipoprotein-B in young men and women. *J. Clin. Endocrinol. Metab.* **96:** E1596–E1605.

31. Cox, L. A., M. Olivier, K. Spradling-Reeves, G. M. Karere, A. G. Comuzzie, and J. L. VandeBerg. 2017. Nonhuman primates and translational research-cardiovascular disease. *ILAR J.* **58:** 235–250.

32. Phillips, M. C. 2014. Apolipoprotein E isoforms and lipoprotein metabolism. *IUBMB Life.* **66:** 616–623.

33. Gordts, P. L., R. Nock, N. H. Son, B. Ramms, I. Lew, J. C. Gonzales, B. E. Thacker, D. Basu, R. G. Lee, A. E. Mullick, et al. 2016. ApoC-III inhibits clearance of triglyceride-rich lipoproteins through LDL family receptors. *J. Clin. Invest.* **126:** 2855–2866.

34. McConathy, W. J., J. C. Gesquiere, H. Bass, A. Tartar, J. C. Fruchart, and C. S. Wang. 1992. Inhibition of lipoprotein lipase activity by synthetic peptides of apolipoprotein C-III. *J. Lipid Res.* **33:** 995–1003.

35. Wang, C. S., W. J. McConathy, H. U. Kloer, and P. Alaupovic. 1985. Modulation of lipoprotein lipase activity by apolipoproteins. Effect of apolipoprotein C-III. *J. Clin. Invest.* **75:** 384–390.

36. Brown, W. V., and M. L. Baginsky. 1972. Inhibition of lipoprotein lipase by an apoprotein of human very low density lipoprotein. *Biochem. Biophys. Res. Commun.* **46:** 375–382.

37. LaRosa, J. C., R. I. Levy, P. Herbert, S. E. Lux, and D. S. Fredrickson. 1970. A specific apoprotein activator for lipoprotein lipase. *Biochem. Biophys. Res. Commun.* **41:** 57–62.

38. Kinnunen, P. K., and C. Ehnholm. 1976. Effect of serum and C-apoproteins from very low density lipoproteins on human postheparin plasma hepatic lipase. *FEBS Lett.* **65:** 354–357.

39. Roth, E. M. 2015. ω-3 carboxylic acids for hypertriglyceridemia. *Expert Opin. Pharmacother.* **16:** 123–133.

40. Soltys, P. A., T. Mazzone, R. W. Wissler, S. Vahed, V. Rangnekar, J. Lukens, D. Vesselinovitch, and G. S. Getz. 1989. Effects of feeding fish oil on the properties of lipoproteins isolated from rhesus monkeys consuming an atherogenic diet. *Atherosclerosis.* **76:** 103–115.

41. Goldstein, J. L., and M. S. Brown. 2015. A century of cholesterol and coronaries: from plaques to genes to statins. *Cell.* **161:** 161–172.

42. Kim, H. J., M. Takahashi, and O. Ezaki. 1999. Fish oil feeding decreases mature sterol regulatory element-binding protein 1 (SREBP-1) by down-regulation of SREBP-1c mRNA in mouse liver. A possible mechanism for down-regulation of lipogenic enzyme mRNAs. *J. Biol. Chem.* **274:** 25892–25898.

43. Deng, X., L. M. Cagen, H. G. Wilcox, E. A. Park, R. Raghow, and M. B. Elam. 2002. Regulation of the rat SREBP-1c promoter in primary rat hepatocytes. *Biochem. Biophys. Res. Commun.* **290:** 256–262.

44. Li, F., W. Zhu, and F. J. Gonzalez. 2017. Potential role of CYP1B1 in the development and treatment of metabolic diseases. *Pharmacol. Ther.* **178:** 18–30.

45. Faeh, D., K. Minehira, J. M. Schwarz, R. Periasamy, S. Park, and L. Tappy. 2005. Effect of fructose overfeeding and fish oil administration on hepatic de novo lipogenesis and insulin sensitivity in healthy men. *Diabetes.* **54:** 1907–1913. [Erratum. 2006. *Diabetes.* 55: 563.]

46. Howell 3rd, G., X. Deng, C. Yellaturu, E. A. Park, H. G. Wilcox, R. Raghow, and M. B. Elam. 2009. N-3 polyunsaturated fatty acids suppress insulin-induced SREBP-1c transcription via reduced trans-activating capacity of LXRalpha. *Biochim. Biophys. Acta.* **1791:** 1190–1196.

JOURNAL OF LIPID RESEARCH